

Computational model of sphingolipids metabolism: a case study of Alzheimer's disease

Agata Charzyńska^{♠,1,2}, Weronika Wronowska^{♠,3}, Karol Nienaltowski⁴, Anna Gambin^{*5,2}

[♠] Equal contributors

¹Institute of Computer Science Polish Academy of Sciences, Warsaw, Poland;

²Bioinformatics Laboratory, Mossakowski Medical Research Centre Polish Academy of Sciences, Warsaw, Poland;

³Faculty of Biology University of Warsaw, Warsaw, Poland;

⁴Institute of Fundamental Technological Research Polish Academy of Sciences, Warsaw, Poland;

⁵Institute of Informatics, University of Warsaw, Warsaw, Poland;

Email: a.charzynska@phd.ipipan.waw.pl; wwro@biol.uw.edu.pl; k.nienaltowski@sysbiosig.org; aniag@mimuw.edu.pl;

* Corresponding author

Abstract

Background: Sphingolipids – as suggested by the prefix in their name – are mysterious molecules, which play surprisingly various roles in opposable cellular processes, like autophagy, apoptosis, proliferation and differentiation. Recently they have been also recognized as important messengers in cellular signalling pathways. More importantly, sphingolipid metabolism disorders were observed in various pathological conditions such as cancer and neurodegeneration.

Results: Existing formal models of sphingolipids metabolism concentrates mostly on *de novo* ceramide synthesis or restrict their focus to biochemical transformations of a particular subspecies. We propose first comprehensive computational model of sphingolipid metabolism in human tissue. In contrast to previous approaches we explicitly model compartmentalization what allows emphasizing the differences among individual organelles.

Conclusions: Presented here model was validated by means of recently proposed model analysis technics allowing for detection of most sensitive and experimentally non-identifiable parameters and determination of main sources of model variance. Moreover, we demonstrate the utility of the model for the study of molecular processes underlying Alzheimer's disease.

1 Background

Sphingolipids (SL) are categorized as a class of complex lipids containing sphingoid base (SPH) [1]. Modification of this basic structure by amide-linked fatty acid or by phosphorylation gives rise to vast family of bioactive sphingolipids like: ceramide (CER), ceramide-1-phosphate(C1P), sphingosine-1-phosphate (S1P) or sphingomyelin (SM) [2,3]. Ceramide is known to be branching point for the metabolism of various sphingolipids subspecies. There are three major pathways of ceramide synthesis. In *de novo* synthesis pathway ceramide is created from less complex molecules [4]. The second path is catabolism of complex sphingolipids, mainly sphingomyelin [5]. Ceramide generation can also occur through the breakdown of complex sphingolipids that are ultimately broken down into sphingosine in acidic environment of lysosome. In this pathway, known as *salvage pathway*, sphingosine is then reused by reacylation to form ceramide [6]. On the same time ceramide may serve as a substrate for the synthesis of SM, C1P, and SPH which, in turns, can be phosphorylated to S1P [7–11]. For the long time these molecules were considered to have mainly structural function, but only in the last two decades sphingolipids were recognized as important messengers in cellular signalling pathways [12,13].

Notable body of work has been devoted studying the influence of sphingolipids metabolism on cellular fate – autophagy, apoptosis, proliferation and differentiation [14,15]. Importantly, individual sphingolipid species appear to have the opposite effect on cell growth and survival. Dynamic balance between proapoptotic molecules (e.g. CER and SPH) and antiapoptotic – prosurvival ones (e.g. S1P and C1P) is termed as *sphingolipid rheostat* [16]. Disruptions in metabolic pathways involved in controlling this balance are considered to underlay various diseases. Indeed, sphingolipids are known to have critical implications for the pathogenesis and treatment of such different illnesses like cancer [17–20] and neurodegenerative disorders (e.g. Alzheimer’s disease) [21–25].

Related research. Formal modelling seems to be an excellent tool to predict the response of the systems in different scenarios and to the wide range of both external and internal perturbations. However, due to the complexity of sphingolipids metabolom, and the paucity of data, not much has been done in the field of computational sphingolipidom modelling. There are only few models of SL metabolism available in the literature. Provided by Vasquez et al. [26] model refers to *de novo* ceramide synthesis in yeast. It captures

all essential elements of the ceramide synthesis from nonsphingolipid metabolites. However, no further steps of ceramide and other more complex sphingolipids recycling (SM catabolic pathway and *salvage pathway*) were taken into consideration.

The model proposed by Gupta et al. [27] describes the C16-branch of sphingolipid metabolism in RAW264.7 cells. An advantage of this model is that it combines lipidomics and transcriptomics data provided by the LIPID MAPS Consortium. However, the model is restricted to the closest metabolites of C16 ceramide. Moreover none of the proposed models captured cell compartmental division, although it is known that the ceramide metabolism differentiates among different cell compartments such as mitochondria, nucleus and cell membrane. Therefore we found the construction of computational model for the metabolism of complex sphingolipids in human tissues to be an appealing task.

Our results. We propose a formal model of regulatory processes capturing sphingolipid metabolism pathways. Computational modelling is based on ordinary differential equations (ODEs) describing the evolution of species concentration. Kinetics of the model is mostly based on the Mass Action Law (MAL) for the molecular transportation reactions and the Michaelis-Menten (MM) approach for enzymatically catalysed reactions. The modelled kinetics also covers the inhibition within competing species.

According to our best knowledge it is the first computational model of sphingolipid metabolism comprising the compartmentalization based on typical structure of non-differentiated eukaryotic cell. Reaction parameters were estimated basing on publicly available literature data and some default assumptions based on experience with Biochemical Systems Theory (BST) [28], while the initial concentrations of particular sphingolipid species in each organelle were taken from the LIPID MAPS database [29]. To validate our model we applied both standard and novel methods of analysis i.e.: the local sensitivity analysis [30], the variance decomposition [31] and the clustering of model's parameters based on sensitivities clusters [32]. Finally we demonstrate the utility of our model to study the molecular events that are known to underly Alzheimer's disease (AD). The proposed model provides a comprehensive, functional integration of experimental data, and we hope it will have significant implications for understanding of still not fully elucidated dependence between sphingolipid metabolism and various diseases. Moreover for the first time the two recently published methods of computational models analysis (i.e. variance decomposition [31] and sensitivity clustering [32]) were applied to the medium size realistic biochemical model.

The ceramides metabolism diagram

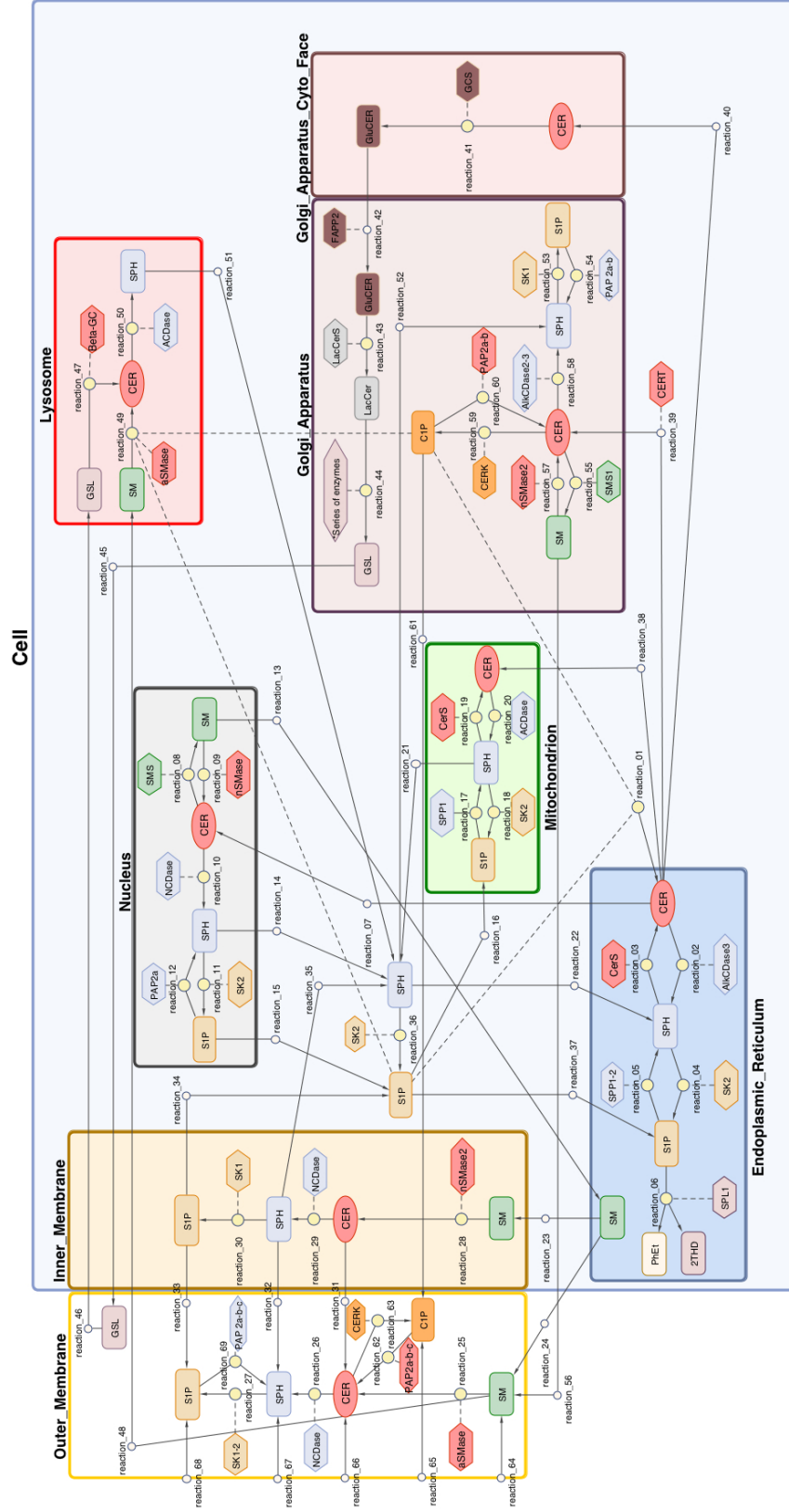


Figure 1: Network of the SL metabolism system. The full model contains 69 reactions, 39 modelled species and 37 reaction catalysing enzymes. Solid lines indicate transportation and enzymatic reactions, dotted lines indicate inhibition.

2 Results and Discussion

2.1 Model of sphingolipids metabolism.

Our model captures all essential elements in the complex network of sphingolipids metabolism, except the *de novo* synthesis of ceramide, which had been described by Vasquez et al. [26]. It illustrates the general behaviour of chosen subspecies in non specified human tissue in 9 sub-cellular compartments representing following organelle or their distinct parts: outer and inner layer of cell membrane, cytoplasm, endoplasmic reticulum, cytoplasmatic and luminal face of Golgi apparatus, nucleus, mitochondria and lysosome. Our model includes 69 reactions of molecular transportation and biochemical transformation, see Figure 1.

Transportation

We applied Mass Action Law principle to describe transportation kinetics. Particular equations simulate different ways of SL transportation, which are determined by specific biophysical properties of particular sphingolipids [33]. It should be mentioned that most of these molecules (i.e. CER, SM, GSL) are restricted to biological membranes. Their transportation between organelle is possible only in form of complexes with lipid transfer proteins (LTP) [34] e.g. ceramide transfer protein (CERT) binds to CER. Additionally, they might change their location in form of vesicles, as an integral part of biological membranes [35]. For example translocation of SM and GSL from Golgi apparatus to outer membrane is correlated with exocytosis, while during the endocytosis complex SL may get in to the lysosome. Sphingolipids may also diffuse along the membranes between linked organelle, as it is in case of ceramide floating between endoplasmic reticulum and nucleus [36]. On the other hand, SPH, S1P and C1P are enough hydrophilic to diffuse freely from the membranes to the cytosol, likewise from the outer membrane to the external environment [37]. Still, it was reported that transportation of C1P from the Golgi apparatus to other cellular compartments may also occur in association with specific transporter proteins as ceramide-1-phosphate transfer protein CPTP [38]. Water solubility also determines molecules ability to flip between membrane leaflets. CER has relatively rapid flip rate, also SPH is sufficiently amphipathic to move between membrane layers [39, 40]. Finally S1P needs specific lipid transporters to traverse membranes [41, 42]. Similarly complex sphingolipids are unable to cross the membranes without the aid of specific flippases like four-phosphate adaptor protein 2 FAPP2 pulling GluCER from the outer to the inner surface of Golgi cisterns [43].

Ceramide synthesis and degradation

Most of the reactions depicted in the diagram are enzymatic. Michaelis-Menten model (MM) and simplified kinetics derived by the MM model was applied to describe different ways of synthesis and degradation of chosen SL species. CER synthesis via *de novo* path is described as the inflow of these molecule in endoplasmic reticulum. CER might be also generated by the acetylation of SPH. This reaction, catalysed by different types of ceramide synthases (CerS) [44] is the final step of the *salvage pathway* [6]. Importantly endoplasmic SPH utilized in this path may become from degradation of S1P what is catalysed by specific phosphatases (SPP1 and SPP2) [45] or from lysosomal degradation of complex SL. This later path initiated by acidic sphingomyelinase (aSMase) and known to be critical for the maintaining proper concentrations of cellular SL [46, 47]. In addition to described above endoplasmic route of CER synthesis similar subset of reactions can be described for the mitochondria. Although, reactions of mitochondrial SL metabolism are not fully understood yet. Especially enzymes specificity and values of reaction rates parameters are often unknown [48, 49]. The third way of CER synthesis is hydrolysis of SM. SMases responsible for catalysing this reaction are classified in to three categories based on their pH optima and sub-cellular distribution. Degradation of SM is known to be essential for the homeostasis of cell membranes, it was also reported to be strongly related to the stress induced apoptosis [14, 50, 51]. Finally we described hydrolysis of CER. Catalysing this reaction ceramidases CDase, 7 of which are known in human, cleave fatty acids from CER producing SPH [52].

Synthesis of complex SL

At the apex of SL complexity are sphingomyelins (SM) and even more diverse glycosphingolipids (GSL). Even though some enzymes responsible for the synthesis of these complex SL were detected in e.g. nucleus this pathway is mainly localized in the Golgi apparatus. In both cases CER is utilized as a backbone molecule. However, whether it would be converted in to SM or GSL depends on the way of its transportation from the endoplasmic reticulum. CER transported in the complex with CERT protein gets to the cis-Golgi where it gives rise to the SM in the SMS catalysed reaction [53, 54]. While, to form GSL in the series reactions CER must get to the trans-Golgi via vesicle dependent way [55].

S1P and C1P metabolism

Moreover our model includes reactions of CER and SPH phosphorylation, produced S1P and C1P, unlike CER and SPH, promote cell growth and have anti-apoptotic properties [16, 56]. The antagonistic effect of

these metabolites is regulated by the activity of many enzymes: (i) ceramide kinase CERK responsible for the synthesis of C1P in the Golgi apparatus and the plasma membrane [57], (ii) sphingosine kinases SK1 and SK2 catalysing phosphorylation of SPH in different subcellular locations [58,59] (iii) mentioned before phosphatases able to hydrolyse S1P and C1P. Among them are both lipid phosphate phosphatases of broad specificity (PAP2a, PAP2b and PAP2c) and S1P specific phosphatases (SPP1 and SPP2) [45,60]. All these enzymes with their isoforms differ in the substrate specificity, optimum pH and sub-cellular localization. Our model illustrates most of their known properties. For detailed characteristics see review articles [7–11]. Importantly both S1P and C1P has been identified as inhibitors of enzymes responsible for CER synthesis like acidic sphingomyelinase (aSMase) and serine palmitoyltransferase (SPT), the key regulatory enzyme of *de novo* synthesis pathway. This inhibitory activity was described in our model by the inhibitory kinetics, for details see supplementary Table 1. Finally our model includes reaction of irreversible degradation of S1P. Catalysed by sphingosine-1-phosphate lyase (SPL1) reaction of S1P hydrolysis to hexadecenal and phosphoethanolamine allows removal of sphingoid base from the pool of SL metabolites [60,61].

Model parameters

To conclude the model consists of 39 variables representing molecular species concentrations (some of them are the same compounds localized in different compartments see Figure 1). Metabolic reactions network covers 69 biochemical enzymatic and transportation reactions among the reacting species. The model is implemented in a form of a system of 69 ordinary differential equations (ODEs) modelling the reaction network dynamics. Relevant input of the model are 129 parameters of inhibition and reactions rates in stationary state representing homeostasis conditions presented in supplementary Table 1 as well as 38 initial values of species concentrations (supplementary Table 2). To achieve conditions resembling intracellular environment during the homeostasis we stabilize the species concentrations to the stationary state of the system. Initial values for lipid levels were taken from the LIPID MAPS [26]. In the sequel, we validate the model by performing local sensitivity analysis, variance decomposition and clustering analysis.

2.2 Computational validation of the model

Biochemical models are characterized by substantially larger number of parameters relative to data size. Therefore the exact estimation of model parameters is very difficult to perform [62]. Thus we used mathematical modelling to analyse the dependencies between parameters and model dynamics. To verify assumptions of our model we applied several techniques to get the broad view of the modelled system

behaviour under normal and stressed conditions. The validation techniques were based on recently proposed and classical approaches engaging exact mathematical methods.

Local sensitivity analysis

The outcome of the local sensitivity analysis [30] performed for system in stationary state – homeostasis (see Figure 2 and supplementary Figures 1-3) yielded the following conclusions.

The local sensitivity analysis of the ceramides species

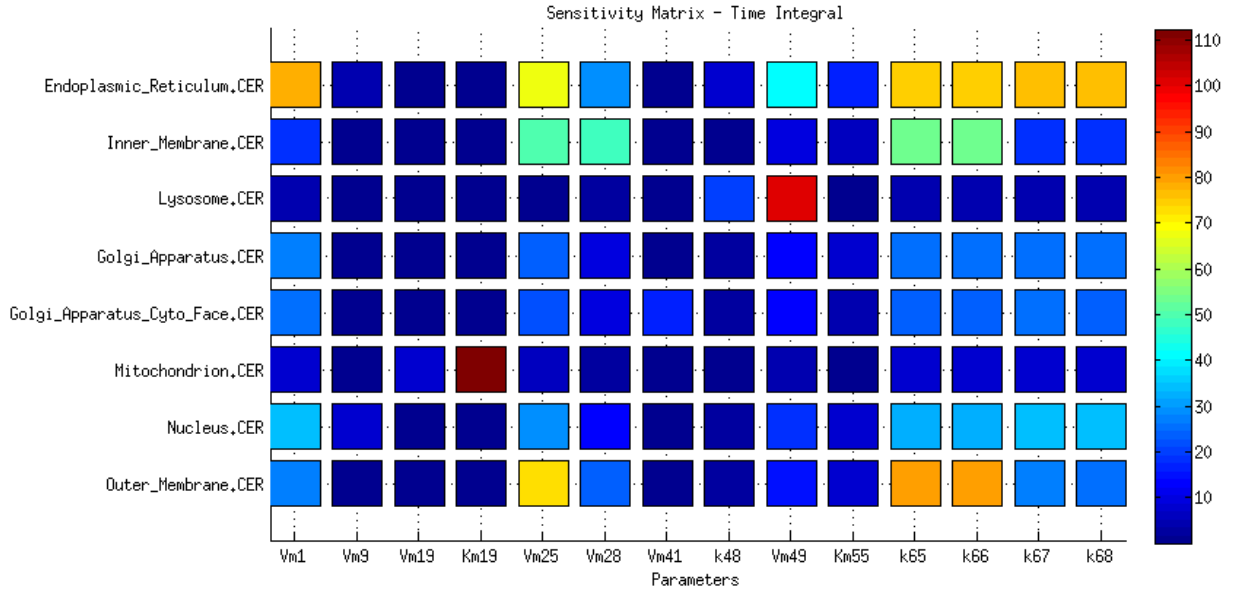


Figure 2: The local sensitivity analysis of the CER species to the highly significant parameters.

- Within ceramide species the highest sensitivity indices were assigned to mitochondrial and lysosomal CER according to ceramide synthase (CerS) in mitochondrion and sphingomyelinase (SMase) in lysosome respectively. The highest variability present CER in endoplasmic reticulum mostly to the model's inflows parameters both the exogenous by outer membrane and endogenous by *de novo* synthesis in endoplasmic reticulum. What is more unexpected CER in endoplasmic reticulum is also highly sensitive to the parameter reaction catalysed by SMase in outer membrane. High sensitivity to the parameters of exogenous inflow of CER and C1P show membrane CER species, which are also sensitive to the membrane reactions catalysed by SMases (see Figure 2).

- For the sphingosine species the greatest instability behaviour shows the mitochondrial SPH, that is highly sensitive to the model's inflows parameters as well as the parameter of reaction catalysed by enzyme CerS in mitochondrion. Moreover mitochondrial SPH is sensitive to the SMase catalysed reactions in membrane (see supplementary Figure 1). In contrary concentration of SPH localised in cytozol is practically invariant to parameters.
- Mitochondrial S1P shows the greatest instability within the S1P species, not only for the model's inflows parameters and CerS in mitochondrion, but also for parameters of reactions catalysed by SMase in membrane and lysosom. For the other S1P species the greatest significant is sphingosinokinase in reticulum, inner membrane and nucleus respectively. Again the cytoplasmic S1P is the most stable S1P species (see supplementary Figure 2).
- Sphingomyelin in outer membrane is the dominant species within all other species, consequently the exogenous inflow of SM by outer membrane is the most significant parameter for the SM species. Other surprising observation is that this parameter does not play noticeable role for all other species that are sensitive for model's inflows parameters by outer membrane (exogenous: C1P, CER, SPH, S1P). Another interesting feature is that the nuclear SM is the most stable within SM species (see supplementary Figure 3).

Variance decomposition – homeostasis

The variance decomposition method [31] enables to decompose noise – the uncertainty of the modelled output into components seaming from different reactions [31,63]. This method applied to our model principally indicate the reactions corresponding to edges in Figure 1 incident to investigated species as the highest noise generators. Nevertheless some reactions were more significant for investigated species than other incident reactions, whereas for some other species variance were distributed equally among all reactions. To find the distinctive reactions we calculated the mean variance for each investigated species and set the threshold to 110% of the mean variance. The results for CER species are depicted in Figure 3 and for SPH, S1P and SM is depicted in supplementary Figures 4-6, respectively.

- Within the ceramides species the highest variance shows the mitochondrial and lysosomal CER. For CER the threshold set on 110% of average variance was exceeded only by the reactions catalysed by ceramideshynthase (CerS) and acid ceramidase (ACDase) in mitochondrion. The membrane CER species interact together so for inner membrane CER not only incident reactions exceeded the

The variance decomposition for the ceramides species

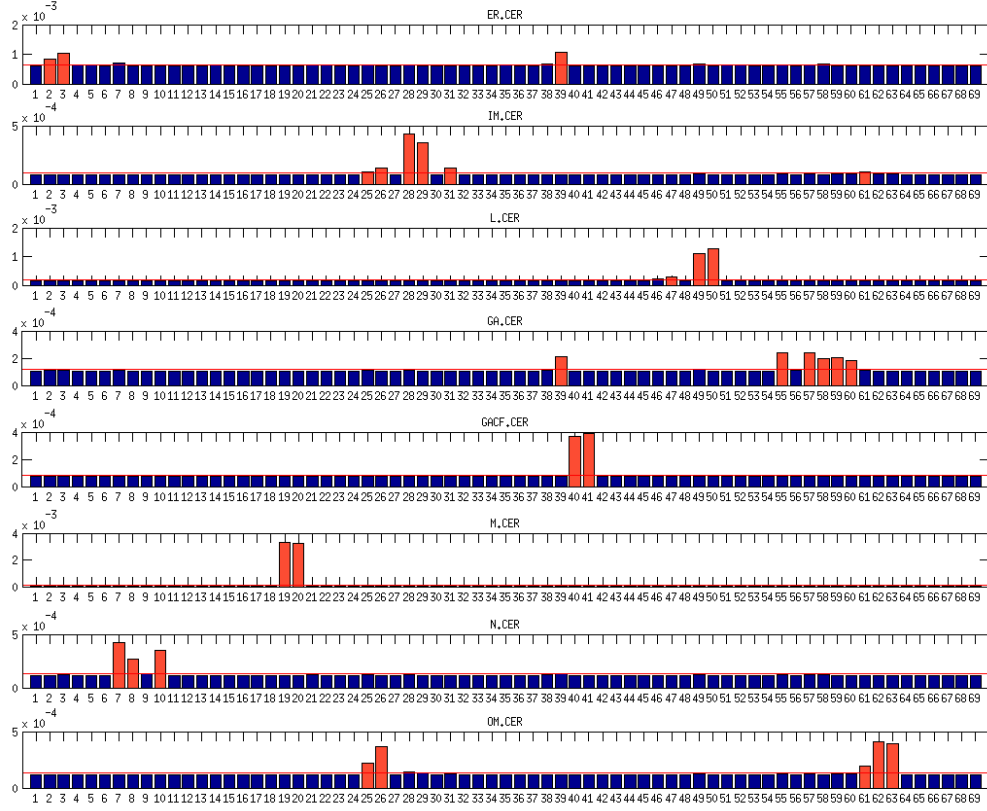


Figure 3: The variance decomposition of the ceramides concentration into components steaming from all model reactions. The red lines denotes the averages variance components of the investigated species. The red bars denotes the variance components that exceed the threshold of 110% of average. The x- axis denotes reactions numbers, the y-axis denotes the size of variance components.

threshold but also reaction incident with outer membrane CER catalysed by aSMase. For the outer membrane CER the highest variance component steams from the reactions incident with outer membrane C1P and transportation reaction of C1P from Golgi apparatus to outer membrane. For the other CER species the highest variance is caused by the incident reactions.

- Within the sphingosine species the highest variance similarly to CER species falls to the mitochondrial SPH, whereas contrary to the mitochondrial CER for the mitochondrial SPH all reactions' noise components are near to the average. Interesting is that two incident reactions

connecting mitochondrial SPH with mitochondrial CER exceeded threshold and two other incident reactions connecting mitochondrial SPH with mitochondrial S1P are significantly below the average. Similarly nuclear and endoplasmic SPH have high and almost equally distributed noise with most significant incident reactions. For nuclear SPH the threshold was exceeded also by non-incident reactions incident with nuclear CER. For the membrane SPH species highly influential reaction is the SPH membrane diffusion. For the inner membrane SPH except the incident reactions the high noise components steams from reactions connected with outer membrane CER (between outer membrane SM and SPH). The outer membrane SPH significant reactions include transportation reaction of C1P from Golgi apparatus to outer membrane and reactions connected with outer membrane CER and outer membrane S1P. For the lysosomal SPH except incident reactions the high noise component steams from reaction catalysed by aSMase in lysosome. For the cytoplasmic SPH except incident reactions the threshold was exceeded by the reaction catalysed by AlkCDase in Golgi apparatus. For Golgi apparatus SPH the noise was mainly decomposed by incident reactions.

- The highest variability within S1P species has the mitochondrial S1P. It's all variance components are near to average noise and non of the reactions exceed the threshold of 110%. Variance of all other S1P species steams principally from the incident reactions with one exception of cytoplasmic S1P which noise is generated mainly by lysosomal reaction catalysed by aSMase.
- The SM species have the highest noise among all species and contrary to most other species the variance of SM species steams almost equally from all reactions.

Sensitivity based parameters clustering (homeostasis)

The complex structure of our model makes it the ideal candidate to test the applicability of new method to detect the mutual relations between parameters via clustering of mutually compensative ones [32]. Usually parameters sets are not pairwise independent and commonly a biochemical model is sensitive to the linear combination of parameters, what makes them not identifiable [62, 64].

Using sensitivity clustering of parameters (see Section Methods 4) we obtained the dendrogram with unequivocal division on four clusters (see Figure 4). We can interpret the obtained clusters as specific functional modules. Importantly, these results are compatible with theoretical compartments recognized by Rao et al. [65], who presented sphingolipid metabolic pathway as a combination of following units: (i) C1 compartment represents the *de novo* biosynthesis of CER, (ii) C2 compartment depicting the conversion of

Parameters clustering based on sensitivities – homeostasis

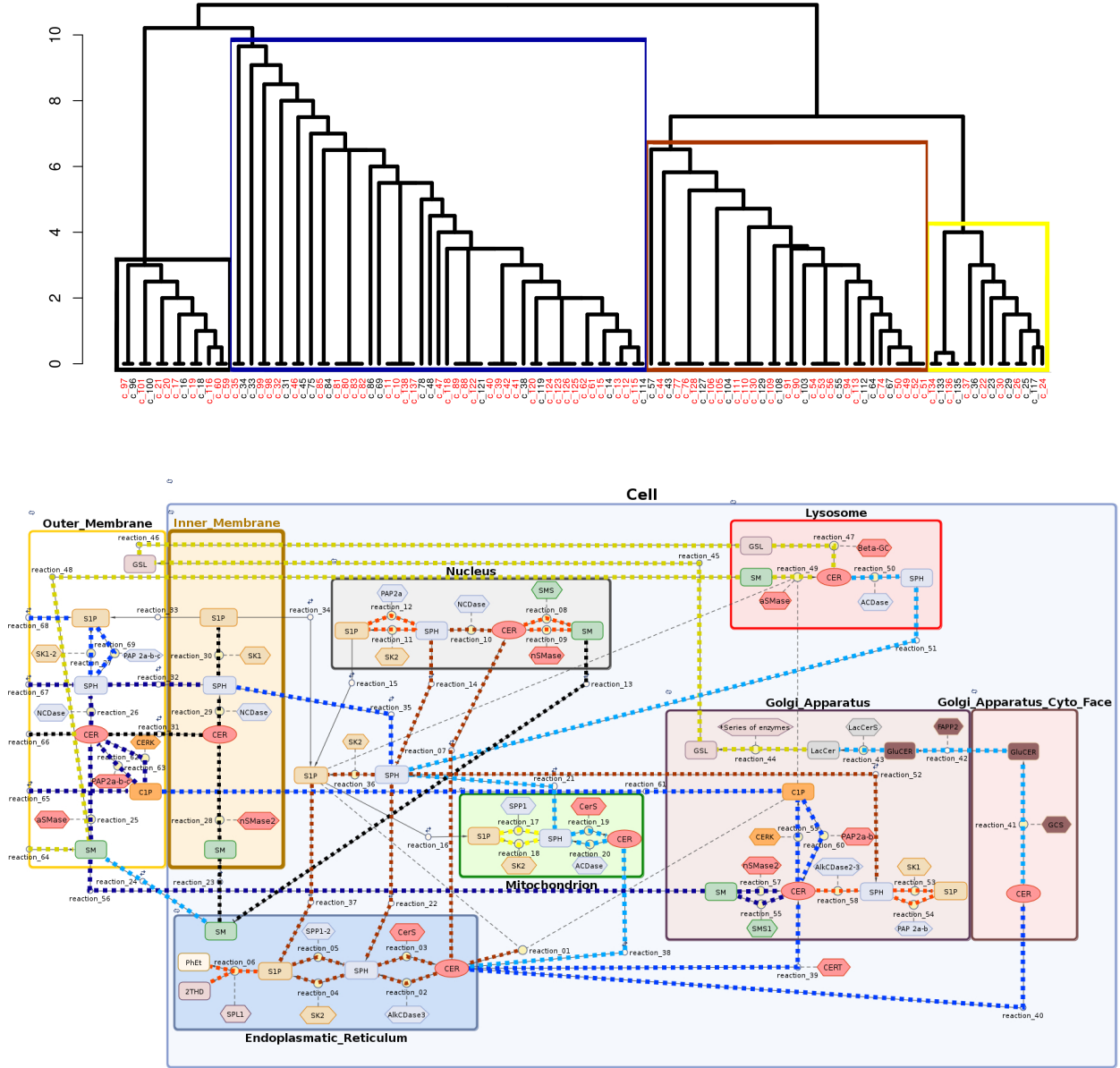


Figure 4: (a) Dendrogram obtained by hierarchical clustering of parameters based on their functional redundancy. Identifiability analysis yielded 37 non-identifiable parameters (marked in red). Correspondence between labels and names of the parameters is given in supplementary materials. (b) Clusters of reactions induced by the hierarchical grouping. Colors of connections between species are compatible with colors of clusters in the dendrogram. Higher color intensity within the cluster means greater level of redundancy between parameters of reaction and other parameters in the cluster.

CER into complex sphingolipid like SM and GSL, (iii) C3 compartment represents hydrolysis of SM to CER, (iv) C4 compartment depicting conversion of CER into bioactive molecules such as C1P and S1P.

Ceramide phosphorylation

The structure of our clusters could be summarized as follows: brown cluster joins reactions parameters from endoplasmic reticulum, Golgi apparatus, nucleus and cytoplasm. Strong redundancy between parameters reflects their functional correlation. This cluster is mostly related to the conversion of SPH to S1P and backwards. Beyond sphingolipids phosphorylation and dephosphorylation it also contains reactions of sphingosine acetylation and reverse reaction – deacetylation of CER. To some extent it corresponds to the C4 compartment described by Rao et al. [65]. However, our cluster does not include reactions taking place in cell membrane, which are classified to the blue and green cluster. Instead, we found reaction depicting endogenous inflow of ceramide in endoplasmic reticulum (simulating the *de novo* synthesis pathway) to be a part of brown cluster. It is worth mention that our analysis shows reactions in endoplasmic reticulum to form functional unity with nuclear reactions. What makes sense as, membranes of reticulum are structurally joined with the nuclear envelope.

Complex SL synthesis

Blue cluster contains reactions parameters related to molecular composition of outer membrane. As cell membrane is the biggest reservoir of sphingolipids, especially complex sphingolipids like sphingomyelin and glycosphingolipids this cluster strongly affects general sphingolipid balance in the cell. Reactions from the pathway of CER production via SM hydrolysis, mentioned before, are localized in this cluster. This is confirmed by local sensitivity analysis, as we can observe strong influence of reaction catalysed by aSMase in outer membrane to many modelled species. As a consequence the pathways responsible for complex sphingolipids (SM and GSL) synthesis are localized in this cluster. These reactions strongly affect stability of endoplasmic CER and subsequently cytoplasmatic SPH. Blue cluster is comparable to the C2 compartment as denoted in [65] reflecting complex SL synthesis. However, extending the results from [65] we have shown that it forms a functional unity with reactions of outer cell membrane. Interestingly results of our simulations are consistent with literature reports as SM metabolism at the plasma membrane is known to have strong implications for bioactive sphingolipids balance [66].

Sphingolipids degradation

Yellow cluster is related to the degradation of complex sphingolipids in acidic environment of lysosome. It includes the starting point of the *salvage pathway* – SM transportation and degradation in lysosome and to some extent resembles the C3 compartment form [65]. According to the local sensitivity analysis two reactions from this cluster representing transportation of SM from outer membrane to lysosome and ceramide synthase from SM in lysosome may affect the concentration of different molecular species of the model like lysosomal and outer membrane CER, SM and SPH, endoplasmic CER or mitochondrial S1P and SPH. However, the strength of this influence is not very high. This finding can be explained by the relatively low activity of lysosomal degradation pathway in cells developing in favourable conditions. It should be mentioned that according to the clustering analysis, lysosome belongs to intersection of yellow and blue clusters what seems biologically correct as this organelle links pathways of complex SL synthesis and degradation.

Inner membrane balance

Black cluster reflects inner membrane molecular balance and contains reaction parameters which are not mutually related with other compartments, but have specific effect on behavior of other pathways. For instance this cluster contains reaction catalysed by nSMase in inner membrane which, on the basis of local sensitivity analysis, appears to have slight impact on the stability of both CER, SPH and S1P in the whole model.

2.3 Application of the model: case study of Alzheimer’s disease

Our model implements not only functional integration of experimental data but may be also used for computational verification of molecular changes known to cause various human diseases. In this study we applied our model to answer the question whether changes in enzymatic activity described by [65] would lead to predicted cell behaviour typical for Alzheimer’s disease (AD). In recent studies it became evident that sphingolipids play important roles in trafficking and metabolism of AD related proteins. Thus, they emerged to crucial molecules in etiology of AD [23, 67]. This devastating neurodegenerative disorder is characterized by the accumulation of intraneuronal and extracellular protein aggregates and progressive synapse loss. Pathological hallmarks of AD are extracellular deposition of peptide termed β -amyloid ($A\beta$) and neurofibrillary tangles. Inability to catabolize aggregates of abnormally folded $A\beta$ leads to neuronal degeneration and subsequent decline in cognitive processes. On the level of sphingolipids metabolism most

frequently reported are ceramide accumulation in endoplasmic reticulum and lysosome and sphingosine accumulation in cytoplasm accompanied by decreased level of cytoplasmatic S1P and C1P [21–25].

Computational simulation of Alzheimer's disease

Aiming to simulate cell response to metabolic disturbances of SL pathway described in [65] we have changed values of chosen reaction parameters for cell homeostasis. For details see supplementary Table 3. We have modified parameters corresponding to the ceramidase (CDase) activity as well as parameters corresponding to sphingosine kinase (SK) and ceramide kinase (CERK) dynamics. Moreover due to down-regulation of CERT expression we have inhibited transportation of CER to Golgi apparatus. On the other hand ceramide *de novo* synthesis reflected by the inflow reaction of CER in endoplasmic reticulum was up-regulated. To test the system response in a AD scenario we simulated the time evolution of species concentrations.

Trajectories of species concentration - AD scenario

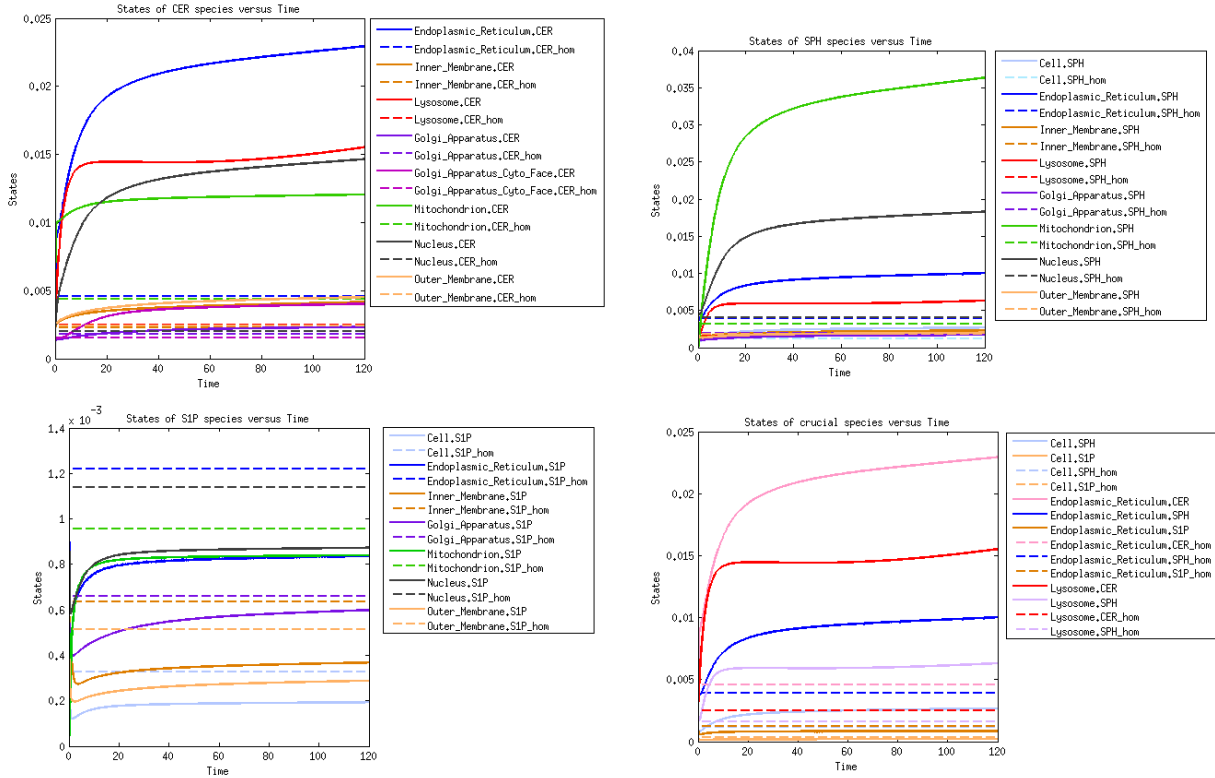


Figure 5: Time evolution of molar concentration for the following groups of species (dashed lines correspond to homeostasis scenario, solid lines to AD scenario): (a) ceramides species; (b) sphingosine species; (c) sphingosine-1-phosphate species; (d) species functionally related to AD.

Preliminary simulations have shown, that when changes were limited to those described by Rao et al. [65] some modelled species quickly diverged to infinity. Namely, we observed unexpected rapid cumulation of SM in many cellular compartments (i.e. lysosome, outer membrane and endoplasmic reticulum). Another unforeseen system behaviour was increased rate of CER to GSL conversion in Golgi Apparatus, followed by accumulation of GSL. Since such events do not occur in AD cells, we suggested that, initially introduced modifications should be accompanied by: (i) reduced transportation of CER to Golgi apparatus via CERT independent pathway, (ii) increased activity of sphingomyelinases (SMase). We also introduced some minor changes in SM transportation between compartments. Importantly our predictions were confirmed by the literature, namely impaired SM metabolism is known to be linked with AD [68,69]. These findings emphasize the predictive value of our model.

After these biologically justified modifications all our results were coherent with experimental data, namely we observed cumulation of ceramides in cellular compartments, especially in endoplasmic reticulum (ER) and lysosome, in comparison to the homeostasis level [65,67].

The model output for sphingosine species concentration showed the imitate drop of SPH species due to CDase down regulation, but than cumulation of SPH species in all compartments as a consequence of the increase of CER species concentration. We also recorded the decrease of S1P species concentration in the AD scenario (see Figure 5).

Local sensitivity analysis for the AD scenario vs homeostasis

Application of the AD scenario yielded slight changes in parameters local sensitivities.

- For the CER species, in contrary to homeostasis, the most sensitive become ceramides in nucleus and endoplasmic reticulum, that are sensitive basically to endogenous CER in endoplasmic reticulum and exogenous C1P, CER, SPH, S1P in outer membrane inflow parameters as well as nSMase reaction rate in outer membrane.
- The S1P in cytosol becomes sensitive to the SK2 in cytosol, analogously S1P in inner membrane becomes sensitive to SK1 in inner membrane and S1P in outer membrane is more sensitive to inflow parameter of exogenous S1P in outer membrane. However the mitochondrial S1P becomes invariant to parameters changes.
- SPH species remains largely unchanged with most sensitive mitochondrial S1P.

- Similarly SM species show an unchanged sensitivity with the dominant species SM in outer membrane most sensitive.

Parameters clustering in the AD scenario vs homeostasis

Clustering analysis of AD model resulted in new parameters dendrogram with only two clusters in comparison to four clusters obtained in homeostasis (see Figure 6 and compare to Figure 4). Clusters distinguished in AD simulation can be described as follows.

Complex SL and GSL metabolism

Green cluster is grouping parameters strongly associated with complex sphingolipids and glycosphingolipids metabolism. It comes out that changes of SM balance are of great importance for cellular metabolism in AD. This cluster includes formation of ceramide on the pathway of SM hydrolysis, catabolism of SM and GSL in lysosome (*salvage pathway*). Similarly to results obtained in homeostasis our model confirms that hydrolysis of SM in cell membrane and lysosome strongly influences the level of cytoplasmic SPH. This cluster also includes parameters related to the synthesis of GSL and SM in Golgi apparatus. To conclude this cluster can be regarded as a combination of green, yellow and a part of the blue homeostatic cluster its formation can be explained by the growth of the importance of SM transportation and degradation during neurodegeneration.

Ceramide synthesis and accumulation

Red cluster includes reactions mostly affected by the inflow of the ceramide from *de novo* synthesis pathway. According to lit. [70] in AD endoplasmic accumulation of ceramide from this source is important step in disease development. Clusters analysis confirmed strong correlation between *de novo* synthesis and concentration of CER in endoplasmic reticulum and subsequently in mitochondrion, nucleus and also Golgi apparatus.

3 Conclusions

In the present paper an original model for sphingolipid metabolism in non-specified human tissue was proposed. To our best knowledge, it is the most comprehensive model so far and also the first one, that explicitly comprises the compartmentalization. We managed to keep the balance between the complexity and biological soundness of the model and its computational tractability.

Parameters clustering based on sensitivities – AD scenario

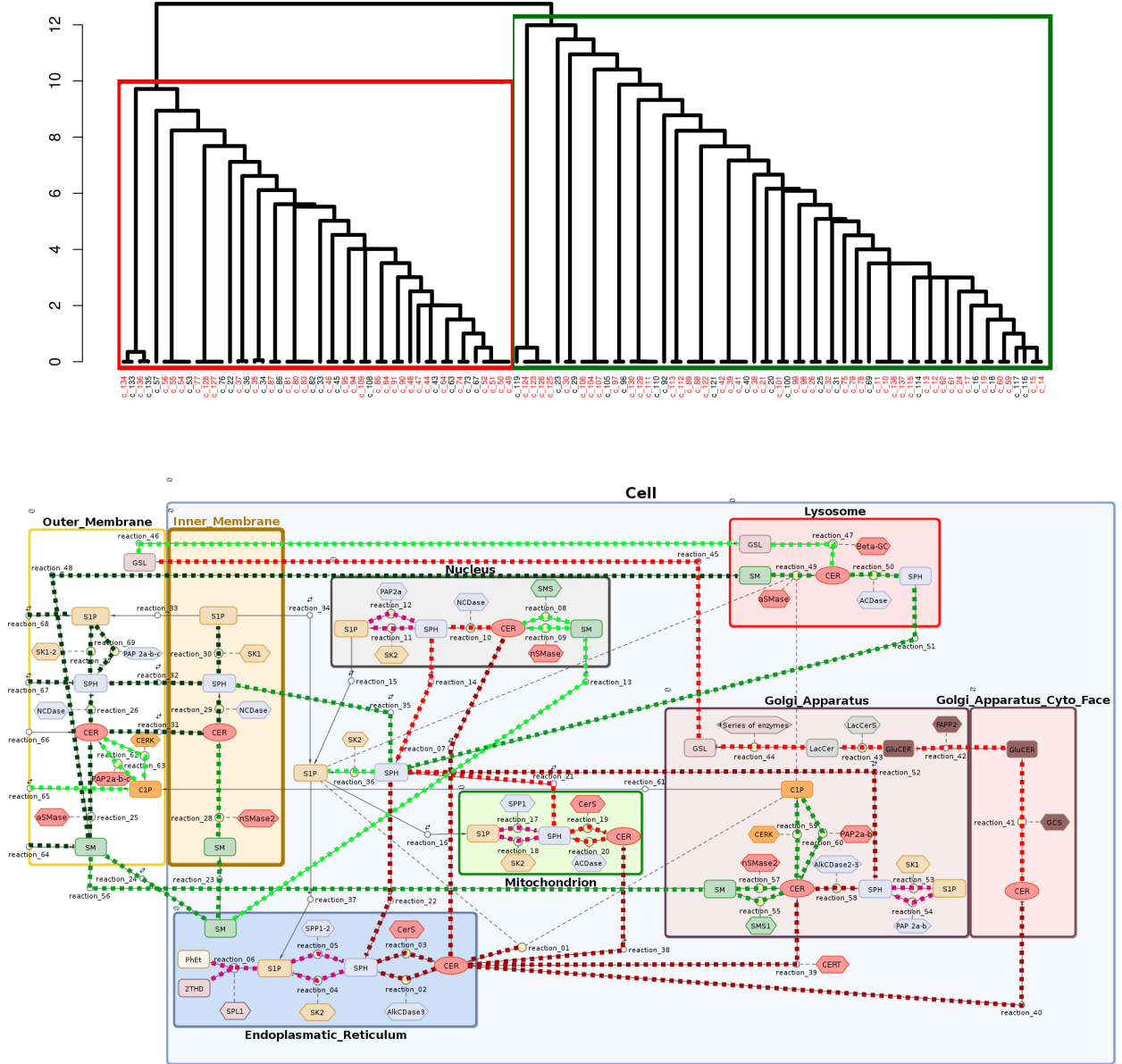


Figure 6: (a) Dendrogram obtained for AD scenario by hierarchical clustering of parameters based on their functional redundancy. Model contains 36 non-identifiable parameters. (b) Clusters of reactions induced by the hierarchical grouping.

Our results demonstrate that the model is an excellent tool for predicting SL pathway reaction to perturbation in activity of particular enzymes, as well as the up- or down-regulation of modeled species.

Thus the model may perfectly be used to simulate molecular behavior in various scenarios as it was shown in the case study of Alzheimer’s disease.

Moreover, the implementation of semi-independent compartments (and the transportation reactions for the molecular species flow between them) allows for more subtle manipulations of the reaction parameters for specific organelle. Finally our model enables not only the integration but also validation of experimental data by verifying their cross-compliance in a complex network of interactions.

Last but not least, the computational validation of the model was performed by means of recently proposed sophisticated approaches [31, 32]. Mathematically elegant methods of variance decomposition and sensitivity clustering of parameters revealed non-trivial biological outcomes. More importantly, at the same time the application of above mentioned approaches to our model constituted the perfect validation of their usefulness in realistic size problems.

4 Methods

All molecular reactions within a system of interacting species $S_1 \dots S_N$ may be presented in the following manner:



where $\underline{\nu}_{nj}$ and $\bar{\nu}_{nj}$ denote amounts of molecules of n -th species that are respectively substrate and product of this reaction and the coefficient k_j denotes reaction rate (speed) of the reaction.

The Mass Action Law kinetics.

In case of non-enzymatic or transpiration kinetics we used the Mass Action Law (MAL) principle. The time derivative of each species concentration is the sum of in- and out-fluxes of all neighbouring reactions. Here the one reaction flux is equal $k_j [S_1]^{\underline{\nu}_{1j}} \dots [S_N]^{\underline{\nu}_{Nj}}$. Hence the Ordinary Differential Equations derived from the MAL can be expressed in the form:

$$\frac{d[S_n]}{dt} = \sum_{j=1}^R s_{nj} k_j [S_1]^{\underline{\nu}_{1j}} \dots [S_N]^{\underline{\nu}_{Nj}} \quad n = 1 \dots N$$

where $s_{nj} = \bar{\nu}_{nj} - \underline{\nu}_{nj}$ denotes a stoichiometric coefficient of n -th species in j -th reaction and $[S_n]$ denotes the concentration of n -th species.

The Michaelis-Menten kinetics.

Most of the reactions depicted in the diagram 1 are enzymatic reactions. For this kind of reactions we used Michaelis-Menten model (MM) and simplified kinetics derived by the MM model:

$$\frac{d[P]}{dt} = \frac{V_{max}[S]}{K_m + [S]},$$

where P denotes reaction product, S denotes reaction substrate and V_{max} , K_m are constant reaction parameters.

Ordinary Differential Equations.

Equivalently the ODEs can be expressed in the matrix form:

$$\frac{d\mathbf{S}(t)}{dt} = M\mathbf{v}(\mathbf{S}(t)),$$

where the system state is represented by the time dependent state vector $\mathbf{S}(t)$ of species concentration, M denotes the stoichiometry matrix and $\mathbf{v}(\mathbf{S}(t))$ denotes a vector of reaction fluxes (in our model according to MAL or MM kinetics including inhibition rates) [30].

4.1 Local Sensitivity Analysis

Local sensitivity analysis shows how the uncertainty of parameters of the model can influence the model output. Sensitivity may be measured by monitoring changes in the output by e.g. partial derivatives of the modelled species to the single parameters. This appears a logical approach as any change observed in the output will unambiguously be due to the single variable changed. To compare the sensitivity of the model to the single parameters one constructs the sensitivity indices by time integration of partial derivatives:

$$s_{n,i} = \int_0^T \left| \frac{\partial S_n(t)}{\partial \theta_i} \right|_{\theta=\theta_0} dt$$

where S_n are different species concentrations, θ is the vector of parameters and θ_0 is some fixed point in parameters space.

4.2 Variance Decomposition

The deterministic approach that represents the mean behaviour of the system can also be generalized to a stochastic mode by means of Stochastic Differential Equations (SDE), both of which can be represented in a discrete Markov Chain or a continuous Markov Process. Below we sketch the method of variance decomposition as presented in [31].

Stochastic Differential Equations.

Modelling the system behaviour in a stochastic manner means the examination not only the evolution of the average system state that represents one of possible trajectories, but examination of the evolution of the probability distribution over all possible system states.

The most popular approach to describe discrete stochastic model of biochemical pathway is Chemical Master Equation (Chapman-Kolmogorov equation of Markov chain modelling the evolution of the system):

$$\frac{dP(\mathbf{x}, t)}{dt} = \sum_j a_j(\mathbf{x} - \mathbf{m}_j)P(\mathbf{x} - \mathbf{m}_j, t) - \sum_j a_j(\mathbf{x})P(\mathbf{x}, t),$$

where the system state is denoted by the vector $\mathbf{X}(t) \in \mathbb{N}^N$ of numbers of molecules each row for one of N reacting species, \mathbf{m}_j denotes the j -th column of stoichiometry matrix $M = (\mathbf{m}_1, \dots, \mathbf{m}_R)$ and $P(\mathbf{x}, t)$ denotes the time- and state-dependent distribution of system being in state $\mathbf{X}(t) = \mathbf{x}$ and finally $a_j(\mathbf{X}(t))$ denotes the propensity function associated with the j -th reaction [30].

One of the possible simplification of the above equation is Linear Noise Approximation, where the dynamic is modelled with Poisson process:

$$\mathbf{X}(t) = \mathbf{X}(0) + \sum_{j=1}^R \mathbf{m}_j N_j \left(\int_0^t f_j(\mathbf{X}(\tau), \tau) d\tau \right)$$

where $N_j(\mathbf{X}(t), t)$ denotes Poisson process dependent on time and a system state $\mathbf{X}(t)$, corresponding to occurrence of j -th reaction. The probability that j -th reaction occur during the time interval $[t; t + dt)$ equals $f_j(x, t)dt$, where the $f_j(x, t)$ is called the transition rate.

Although accurate discrete models describe the exact evolution of probability distribution of the system with the assumption that in one time point at most one reaction can occur, they are computationally not efficient, as simulations require significant resources. Consequently it is more efficient to transit from discrete to continuous process. Starting from deterministic approximation:

$$\Phi(t) = \Phi(0) + \sum_{j=1}^R m_j \int_0^t f_j(\Phi(s), s) ds$$

where $\Phi(t)$ is the mean system state being the solution of the ODEs one can describe the system state evolution by dividing it into deterministic and stochastic part:

$$x(t) = \xi(t) + \Phi(t)$$

where $\Phi(t)$ is the deterministic part and $\xi(t)$ is the Wiener process describing stochastic noise of a system state [71]. The next step of stochastic noise decomposition is to divide noise linearly into noise stemming

from separate reactions. The fact, that the total variance:

$$\Sigma(t) = \langle (x(t) - \langle x(t) \rangle)(x(t) - \langle x(t) \rangle)^T \rangle$$

is described by the differential equation

$$\frac{d\Sigma}{dt} = A(t)\Sigma + \Sigma A(t)^T + D(t), \quad (1)$$

where

$$\{A(\Phi, t)\}_{ik} = \sum_{j=1}^r m_{ij} \frac{\partial f_j(\Phi, t)}{\partial \Phi_k}$$

and $D(t)$ denotes diffusion matrix, can be represented as the sum of individual contributions,

$$\Sigma(t) = \Sigma^{(1)}(t) + \dots + \Sigma^{(r)}(t). \quad (2)$$

results directly from the decomposition of the diffusion matrix $D(t) = \sum_{j=1}^r D^{(j)}(t)$ and the linearity of the equation for $\Sigma(t)$. [31] By decomposing variance into the components from individual reactions, we are able to determine the variability that the model has from each reaction, and therefore we are able to assess and weigh the uncertainty of the model in division into single reactions.

4.3 Parameters clustering

In [32] the concept of *functional redundancy* has been proposed and used in hierarchical clustering algorithm as dissimilarity measure. Let us define the model in Bayesian approach by the distribution of data ($X \in \mathbb{R}^k$) given parameters ($\theta \in \mathbb{R}^l$) as $P(X|\theta)$, together with a *priori* distribution $P(\theta)$. Assume that $\theta = (\theta_A, \theta_B)$ corresponds to division of parameters on two independent sets then [72]:

$$H(X) = I(X, \theta_A) + I(X, \theta_B) + I(\theta_A, \theta_B|X) + H(X|\theta), \quad (3)$$

where H denotes here the entropy and I is the mutual information between random variables. Here $I(\theta_A, \theta_B|X)$ measures this part of entropy which is shared by both sets of parameters and it is equivalent to redundant knowledge of the model which is owned by θ_A and θ_B .

Computation of $I(\theta_A, \theta_B|X)$ requires calculation integral over all possible outcomes of the model what is highly inefficient, hence, this notion has been replaced with local redundancy measure which substitute assumption of knowledge about the model X with information about initial parameters θ^* . Thus, functional redundancy is equal to $I(\theta_A, \theta_B|\theta^*)$ and is calculated according to the formul [73]:

$$I(\theta_A, \theta_B|\theta^*) = -\frac{1}{2} \sum_{i=1}^{\min(|\theta_A|, |\theta_B|)} \log(1 - \rho_j^2), \quad (4)$$

where ρ_i stands for the canonical correlation obtained from the Fisher Information Matrix of θ^* ($FIM(\theta^*)$). Moreover, to indicate *non-identifiable* parameters authors define term of (δ, ζ) - identifiability using the idea of functional redundancy [32]. In this terminology θ_i is (δ, ζ) - identifiable if $FIM_{ii}(\theta) > \zeta$ and $\rho(\theta_i, \theta_{-i}) < 1 - \delta$, where θ_{-i} represents all parameters except θ_i .

Using functional redundancy we can cluster parameters according to hierarchical algorithm (i.e. in every turn of the loop we merge two sets of the parameters with the biggest redundancy measure and remove all nonidentifiable parameters from further analysis) and visualize it on a dendrogram.

Authors contributions

WW designed the biochemical model, AC and KN implemented it and carried out the computational experiments. AG inspired the research and supervised the project. All authors contributed to the writing of this manuscript and have read and approved the final manuscript.

Competing interests

The authors declare that they have no competing interests.

Acknowledgements

All authors thank prof. Bogdan Lesyng and prof. Robert Strosznajder (Mossakowski Medical Center, Polish Academy of Sciences) for valuable discussions and for inspiring this research and, above all – Michał Komorowski for acquainting us with the model analysis methods. This work was partially supported by Polish National Science Center grant n° 2011/01/B/NZ2/00864, Biocentrum-Ochota project (POIG 02.03.00-00-003/09) and EU project POKL.04.01.01-00-051/10-00.

Abbreviations

Abbreviation	Meaning
ACDase	Acidic Ceramidase.
AD	Alzheimer's Disease.
AlkCDase	Alkaline Ceramidase.
aSMase	Acid Sphingomyelinase.
BST	Biochemical Systems Theory.
C1P	Ceramide-1-Phosphate.
CDase	Ceramidase.
CER	Ceramide.
CERK	Ceramide Kinase.
CerS	Ceramide Synthase.
CERT	Ceramide Transfer Protein.
CPTP	Ceramide-1-Phosphate Transfer Protein.
ER	Endoplasmatic Reticulum.
FAPP2	Four-Phosphate Adaptor Protein 2.
GluCER	Glucosylceramide.
GSL	Glycosphingolipid.
LTP	Lipid-Transfer Proteins.
MAL	Mass Action Law kinetics.
MM	Michealis-Menten kinetics.
nSMase	Neutral Sphingomyelinase.
ODEs	Ordinary Differential Equations.
PAP2a	Phosphatidic acid phosphatase type 2a.
PAP2b	Phosphatidic acid phosphatase type 2b.
PAP2c	Phosphatidic acid phosphatase type 2c.
S1P	Sphingosine-1-Phosphate.
SDE	Stochastic Differential Equations.
SK	Sphingosine Kinase.
SK1	Sphingosine Kinase 1.
SK2	Sphingosine Kinase 2.
SL	Sphingolipids.
SM	Sphingomyelin.
SMase	Sphingomyelinase.
SMS	Sphingomyelin Synthase.
SPH	Sphingosine.
SPL1	Sphingosine 1-Phosphate Lyase 1.
SPP1	Sphingosine-1-Phosphate Phosphatase 1.
SPP2	Sphingosine-1-Phosphate Phosphatase 2.
SPT	Serine Palmitoyltransferase.

References

1. Thudichum JLW: *A Treatise on the Chemical Constitution of Brain*. London: Bailliere, Tindall, and Cox 1884.
2. Carter HE, Haines WJ: **Biochemistry of the sphingolipides; preparation of sphingolipides from beef brain and spinal cord**. *J. Biol. Chem.* 1947, **169**:77–82.
3. Pruett ST, Bushnev A, Hagedorn K, Adiga M, Haynes CA, Sullards MC, Liotta DC, Merrill AH: **Biodiversity of sphingoid bases ("sphingosines") and related amino alcohols**. *J. Lipid Res.* 2008, **49**(8):1621–1639.
4. Merrill AH: **De novo sphingolipid biosynthesis: a necessary, but dangerous, pathway**. *J. Biol. Chem.* 2002, **277**(29):25843–25846.
5. Furst W, Sandhoff K: **Activator proteins and topology of lysosomal sphingolipid catabolism**. *Biochim. Biophys. Acta* 1992, **1126**:1–16.
6. Kitatani K, Idkowiak-Baldys J, Hannun YA: **The sphingolipid salvage pathway in ceramide metabolism and signaling**. *Cell. Signal.* 2008, **20**(6):1010–1018.
7. Kolter T, Proia RL, Sandhoff K: **Combinatorial ganglioside biosynthesis**. *J. Biol. Chem.* 2002, **277**(29):25859–25862.
8. Hannun YA, Obeid LM: **Principles of bioactive lipid signalling: lessons from sphingolipids**. *Nat. Rev. Mol. Cell Biol.* 2008, **9**(2):139–150.
9. Gault CR, Obeid LM, Hannun YA: **An overview of sphingolipid metabolism: from synthesis to breakdown**. *Adv. Exp. Med. Biol.* 2010, **688**:1–23.
10. Bartke N, Hannun YA: **Bioactive sphingolipids: metabolism and function**. *J. Lipid Res.* 2009, **50** Suppl:S91–96.
11. Merrill AH: **Sphingolipid and glycosphingolipid metabolic pathways in the era of sphingolipidomics**. *Chem. Rev.* 2011, **111**(10):6387–6422.
12. Hannun YA, Loomis CR, Merrill AH, Bell RM: **Sphingosine inhibition of protein kinase C activity and of phorbol dibutyrate binding in vitro and in human platelets**. *J. Biol. Chem.* 1986, **261**(27):12604–12609.
13. Dressler KA, Mathias S, Kolesnick RN: **Tumor necrosis factor- α activates the sphingomyelin signal transduction pathway in a cell-free system**. *Science* 1992, **255**(5052):1715–1718.
14. Hannun YA: **Functions of ceramide in coordinating cellular responses to stress**. *Science* 1996, **274**(5294):1855–1859.
15. Hannun YA, Obeid LM: **The Ceramide-centric universe of lipid-mediated cell regulation: stress encounters of the lipid kind**. *J. Biol. Chem.* 2002, **277**(29):25847–25850.
16. Cu villier O, Pirianov G, Kleuser B, Vanek PG, Coso OA, Gutkind S, Spiegel S: **Suppression of ceramide-mediated programmed cell death by sphingosine-1-phosphate**. *Nature* 1996, **381**(6585):800–803.
17. Ogretmen B, Hannun YA: **Biologically active sphingolipids in cancer pathogenesis and treatment**. *Nat. Rev. Cancer* 2004, **4**(8):604–616.
18. Ponnusamy S, Meyers-Needham M, Senkal CE, Saddoughi SA, Sentelle D, Selvam SP, Salas A, Ogretmen B: **Sphingolipids and cancer: ceramide and sphingosine-1-phosphate in the regulation of cell death and drug resistance**. *Future Oncol* 2010, **6**(10):1603–1624.
19. Ryland LK, Fox TE, Liu X, Loughran TP, Kester M: **Dysregulation of sphingolipid metabolism in cancer**. *Cancer Biol. Ther.* 2011, **11**(2):138–149.
20. Beckham TH, Cheng JC, Marrison ST, Norris JS, Liu X: **Interdiction of sphingolipid metabolism to improve standard cancer therapies**. *Adv. Cancer Res.* 2013, **117**:1–36.
21. He X, Huang Y, Li B, Gong CX, Schuchman EH: **Deregulation of sphingolipid metabolism in Alzheimer's disease**. *Neurobiol. Aging* 2010, **31**(3):398–408.
22. Haughey NJ, Bandaru VV, Bae M, Mattson MP: **Roles for dysfunctional sphingolipid metabolism in Alzheimer's disease neuropathogenesis**. *Biochim. Biophys. Acta* 2010, **1801**(8):878–886.

23. van Echten-Deckert G, Walter J: **Sphingolipids: critical players in Alzheimer's disease.** *Prog. Lipid Res.* 2012, **51**(4):378–393.
24. Grimm MO, Zimmer VC, Lehmann J, Grimm HS, Hartmann T: **The impact of cholesterol, DHA, and sphingolipids on Alzheimer's disease.** *Biomed Res Int* 2013, **2013**:814390.
25. Ceccom J, Loukh N, Lauwers-Cances V, Touriol C, Nicaise Y, Gentil C, Uro-Coste E, Pitson S, Maurage CA, Duyckaerts C, Cuvillier O, Delisle MB: **Reduced sphingosine kinase-1 and enhanced sphingosine 1-phosphate lyase expression demonstrate deregulated sphingosine 1-phosphate signaling in Alzheimer's disease.** *Acta Neuropathol Commun* 2014, **2**:12.
26. Alvarez-Vasquez F, Sims KJ, Cowart LA, Okamoto Y, Voit EO, Hannun YA: **Simulation and validation of modelled sphingolipid metabolism in *Saccharomyces cerevisiae*.** *Nature* 2005, **433**(7024):425–430.
27. Gupta S, Maurya MR, Merrill AH, Glass CK, Subramaniam S: **Integration of lipidomics and transcriptomics data towards a systems biology model of sphingolipid metabolism.** *BMC Syst Biol* 2011, **5**:26.
28. Sorribas A, Savageau MA: **Sphingolipid metabolic pathway: an overview of major roles played in human diseases.** *Mathematical Biosciences* 1989, **94**(2):161–193.
29. **LIPID MAPS Lipidomics Gateway** [<http://www.lipidmaps.org/>].
30. Charzyńska A, Nalecz A, Rybiński M, Gambin A: **Sensitivity analysis of mathematical models of signaling pathways.** *BioTechnologia* 2012, **93**(3):291–30.
31. Komorowski M, Miekisz J, Stumpf M: **Decomposing Noise in Biochemical Signalling Systems Highlights the Role of Protein Degradation.** *Biophysical Journal* 2013, **104**(8):1783–1793.
32. Włodarczyk M, Lipniacki T, Komorowski M: **Functional redundancy in the NF- κ B signalling pathway** 2013, [<http://arxiv.org/abs/1303.3109>]. [Manuscript submitted for publication].
33. Sonnino S, Prinetti A, Mauri L, Chigorno V, Tettamanti G: **Dynamic and structural properties of sphingolipids as driving forces for the formation of membrane domains.** *Chem. Rev.* 2006, **106**(6):2111–2125.
34. Lev S: **Non-vesicular lipid transport by lipid-transfer proteins and beyond.** *Nat. Rev. Mol. Cell Biol.* 2010, **11**(10):739–750.
35. van Meer G, Lisman Q: **Sphingolipid transport: rafts and translocators.** *J. Biol. Chem.* 2002, **277**(29):25855–25858.
36. Eggeling C, Ringemann C, Medda R, Schwarzmann G, Sandhoff K, Polyakova S, Belov VN, Hein B, von Middendorff C, Schönl A, Hell SW: **Direct observation of the nanoscale dynamics of membrane lipids in a living cell.** *Nature* 2009, **457**(7233):1159–1162.
37. Tani M, Ito M, Igarashi Y: **Ceramide/sphingosine/sphingosine 1-phosphate metabolism on the cell surface and in the extracellular space.** *Cell. Signal.* 2007, **19**(2):229–237.
38. Simanshu DK, Kamlekar RK, Wijesinghe DS, Zou X, Zhai X, Mishra SK, Molotkovsky JG, Malinina L, Hinchcliffe EH, Chalfant CE, Brown RE, Patel DJ: **Non-vesicular trafficking by a ceramide-1-phosphate transfer protein regulates eicosanoids.** *Nature* 2013, **500**(7463):463–467.
39. Contreras FX, Basanez G, Alonso A, Herrmann A, Goni FM: **Asymmetric addition of ceramides but not dihydroceramides promotes transbilayer (flip-flop) lipid motion in membranes.** *Biophys. J.* 2005, **88**:348–359.
40. van Meer G: **Dynamic transbilayer lipid asymmetry.** *Cold Spring Harb Perspect Biol* 2011, **3**(5).
41. Kobayashi N, Kobayashi N, Yamaguchi A, Nishi T: **Characterization of the ATP-dependent sphingosine 1-phosphate transporter in rat erythrocytes.** *J. Biol. Chem.* 2009, **284**(32):21192–21200.
42. Aye IL, Singh AT, Keelan JA: **Transport of lipids by ABC proteins: interactions and implications for cellular toxicity, viability and function.** *Chem. Biol. Interact.* 2009, **180**(3):327–339.
43. D'Angelo G, Polishchuk E, Di Tullio G, Santoro M, Di Campli A, Godi A, West G, Bielawski J, Chuang CC, van der Spoel AC, Platt FM, Hannun YA, Polishchuk R, Mattijus P, De Matteis MA: **Glycosphingolipid synthesis requires FAPP2 transfer of glucosylceramide.** *Nature* 2007, **449**(7158):62–67.

44. Levy M, Futerman AH: **Mammalian ceramide synthases.** *IUBMB Life* 2010, **62**(5):347–356.
45. Brindley DN: **Lipid phosphate phosphatases and related proteins: signaling functions in development, cell division, and cancer.** *J. Cell. Biochem.* 2004, **92**(5):900–912.
46. Jenkins RW, Canals D, Hannun YA: **Roles and regulation of secretory and lysosomal acid sphingomyelinase.** *Cell. Signal.* 2009, **21**(6):836–846.
47. Kolter T, Sandhoff K: **Principles of lysosomal membrane digestion: stimulation of sphingolipid degradation by sphingolipid activator proteins and anionic lysosomal lipids.** *Annu. Rev. Cell Dev. Biol.* 2005, **21**:81–103.
48. Siskind LJ: **Mitochondrial ceramide and the induction of apoptosis.** *J. Bioenerg. Biomembr.* 2005, **37**(3):143–153.
49. Bionda C, Portoukalian J, Schmitt D, Rodriguez-Lafrasse C, Ardail D: **Subcellular compartmentalization of ceramide metabolism: MAM (mitochondria-associated membrane) and/or mitochondria?** *Biochem. J.* 2004, **382**(Pt 2):527–533.
50. Santana P, Pena LA, Haimovitz-Friedman A, Martin S, Green D, McLoughlin M, Cordon-Cardo C, Schuchman EH, Fuks Z, Kolesnick R: **Acid sphingomyelinase-deficient human lymphoblasts and mice are defective in radiation-induced apoptosis.** *Cell* 1996, **86**(2):189–199.
51. Pena LA, Fuks Z, Kolesnick R: **Stress-induced apoptosis and the sphingomyelin pathway.** *Biochem. Pharmacol.* 1997, **53**(5):615–621.
52. Mao C, Obeid LM: **Ceramidases: regulators of cellular responses mediated by ceramide, sphingosine, and sphingosine-1-phosphate.** *Biochim. Biophys. Acta* 2008, **1781**(9):424–434.
53. Merrill AH, Jones DD: **An update of the enzymology and regulation of sphingomyelin metabolism.** *Biochim. Biophys. Acta* 1990, **1044**:1–12.
54. Tafesse FG, Ternes P, Holthuis JC: **The multigenic sphingomyelin synthase family.** *J. Biol. Chem.* 2006, **281**(40):29421–29425.
55. Funato K, Riezman H: **Vesicular and nonvesicular transport of ceramide from ER to the Golgi apparatus in yeast.** *J. Cell Biol.* 2001, **155**(6):949–959.
56. Cu villier O, Pirianov G, Kleuser B, Vanek PG, Coso OA, Gutkind S, Spiegel S: **Suppression of ceramide-mediated programmed cell death by sphingosine-1-phosphate.** *Nature* 1996, **381**(6585):800–803.
57. Sugiura M, Kono K, Liu H, Shimizugawa T, Minekura H, Spiegel S, Kohama T: **Ceramide kinase, a novel lipid kinase. Molecular cloning and functional characterization.** *J. Biol. Chem.* 2002, **277**(26):23294–23300.
58. Maceyka M, Payne SG, Milstien S, Spiegel S: **Sphingosine kinase, sphingosine-1-phosphate, and apoptosis.** *Biochim. Biophys. Acta* 2002, **1585**(2-3):193–201.
59. Pitson SM: **Regulation of sphingosine kinase and sphingolipid signaling.** *Trends Biochem. Sci.* 2011, **36**(2):97–107.
60. Spiegel S, Milstien S: **Sphingosine-1-phosphate: an enigmatic signalling lipid.** *Nat. Rev. Mol. Cell Biol.* 2003, **4**(5):397–407.
61. Bourquin F, Riezman H, Capitani G, Grutter MG: **Structure and function of sphingosine-1-phosphate lyase, a key enzyme of sphingolipid metabolism.** *Structure* 2010, **18**(8):1054–1065.
62. Brown KS, Sethna JP: **Statistical mechanical approaches to models with many poorly known parameters.** *Physical Review E - PHYS REV E* 2003, **68**(2).
63. Jetka T, Charzyńska A, Gambin A, Stumpf MP, Komorowski M: **StochDecomp - Matlab package for noise decomposition in stochastic biochemical systems.** *Bioinformatics* 2014, **30**:137–138.
64. Lipniacki T, Paszek P, Brasier AR, Luxon B, Kimmel M: **Mathematical model of NF- κ B regulatory module.** *Journal of theoretical biology* 2004, **228**(2):195–215.
65. Pralhada Rao R, Vaidyanathan N, Rengasamy M, Mammen Oommen A, Somaiya N, Jagannath MR: **Sphingolipid metabolic pathway: an overview of major roles played in human diseases.** *J Lipids* 2013, **2013**:178910.

66. Milhas D, Clarke CJ, Hannun YA: **Sphingomyelin metabolism at the plasma membrane: implications for bioactive sphingolipids.** *FEBS Lett.* 2010, **584**(9):1887–1894.
67. Di Paolo G, Kim TW: **Linking lipids to Alzheimer’s disease: cholesterol and beyond.** *Nat. Rev. Neurosci.* 2011, **12**(5):284–296.
68. Jana A, Pahan K: **Fibrillar amyloid-beta-activated human astroglia kill primary human neurons via neutral sphingomyelinase: implications for Alzheimer’s disease.** *J. Neurosci.* 2010, **30**(38):12676–12689.
69. Lee JK, Jin HK, Park MH, Kim BR, Lee PH, Nakauchi H, Carter JE, He X, Schuchman EH, Bae JS: **Acid sphingomyelinase modulates the autophagic process by controlling lysosomal biogenesis in Alzheimer’s disease.** *J. Exp. Med.* 2014, **211**(8):1551–1570.
70. Paschen W, Mengesdorf T: **Endoplasmic reticulum stress response and neurodegeneration.** *Cell Calcium* 2005, **38**(3-4):409–415.
71. Komorowski M, Finkenstadt B, Harper CV, Rand DA: **Bayesian inference of biochemical kinetic parameters using the linear noise approximation.** *BMC Bioinformatics* 2009, **10**:343.
72. Lüdtke N, Panzeri S, Brown M, Broomhead DS, Knowles J, Montemurro MA, Kell DB: **Information-theoretic sensitivity analysis: a general method for credit assignment in complex networks.** *Journal of The Royal Society Interface* 2008, **5**(19):223–235.
73. Johnson R, Wichern D: *Applied multivariate statistical analysis, volume 4.* NJ: Prentice hall Englewood Cliffs 1992.